J. Fluid Mech. (1999), *vol.* 384, *pp.* 107–132. Printed in the United Kingdom

The turbulent burning velocity for large-scale and small-scale turbulence

By N. PETERS

Institut für Technische Mechanik, RWTH Aachen, 52056 Aachen, Germany

(Received 16 October 1997 and in revised form 29 October 1998)

The level-set approach is applied to a regime of premixed turbulent combustion where the Kolmogorov scale is smaller than the flame thickness. This regime is called the thin reaction zones regime. It is characterized by the condition that small eddies can penetrate into the preheat zone, but not into the reaction zone.

By considering the iso-scalar surface of the deficient-species mass fraction Y immediately ahead of the reaction zone a field equation for the scalar quantity $G(\boldsymbol{x}, t)$ is derived, which describes the location of the thin reaction zone. It resembles the level-set equation used in the corrugated flamelet regime, but the resulting propagation velocity s_L^* normal to the front is a fluctuating quantity and the curvature term is multiplied by the diffusivity of the deficient species rather than the Markstein diffusivity. It is shown that in the thin reaction zones regime diffusive effects are dominant and the contribution of s_L^* to the solution of the level-set equation is small.

In order to model turbulent premixed combustion an equation is used that contains only the leading-order terms of both regimes, the previously analysed corrugated flamelets regime and the thin reaction zones regime. That equation accounts for non-constant density but not for gas expansion effects within the flame front which are important in the corrugated flamelets regime. By splitting G into a mean and a fluctuation, equations for the Favre mean $\widetilde{G}$ and the variance $\widetilde{G''^2}$ are derived. These quantities describe the mean flame position and the turbulent flame brush thickness, respectively. The equation for $\widetilde{G''^2}$ is closed by considering two-point statistics. Scaling arguments are then used to derive a model equation for the flame surface area ratio $\tilde{\sigma}$. The balance between production, kinematic restoration and dissipation in this equation leads to a quadratic equation for the turbulent burning velocity. Its solution shows the 'bending' behaviour of the turbulent to laminar burning velocity ratio s_T/s_L, plotted as a function of v'/s_L. It is shown that the bending results from the transition from the corrugated flamelets to the thin reaction zones regimes. This is equivalent to a transition from Damköhler's large-scale to his small-scale turbulence regime.

1. Introduction

Damköhler (1940) was the first to present theoretical expressions for the turbulent burning velocity. He identified two different regimes which he called large-scale and small-scale turbulence, respectively. For large-scale turbulence he assumed that the interaction between a wrinkled flame front and the turbulent flow field is purely kinematic and therefore independent of lengthscales. This corresponds to the corrugated flamelets regime which has been discussed previously (cf. Peters 1986; Bray 1996). Damköhler equated the mass flux $\dot{m}$ of unburnt gas with the laminar burning

velocity s_L through the turbulent flame surface area F_T to the mass flux through the cross-sectional area F with the turbulent burning velocity s_T

$$\dot{m} = \rho_u s_L F_T = \rho_u s_T F. \tag{1.1}$$

Here ρ_u is the density of the unburnt mixture. The burning velocities s_L and s_T are also defined with respect to the conditions in the unburnt mixture. This leads to

$$\frac{s_T}{s_L} = \frac{F_T}{F}. \tag{1.2}$$

Using the geometrical analogy with a Bunsen flame, Damköhler assumed that the area increase of the wrinkled flame surface area relative to the cross-sectional area is proportional to the increase of flow velocity over the laminar burning velocity

$$\frac{F_T}{F} = \frac{s_L + v'}{s_L}. \tag{1.3}$$

Here v' is the velocity increase which finally is identified as the r.m.s. velocity v'. Combining (1.2) and (1.3) leads to

$$\frac{s_T}{s_L} = 1 + \frac{v'}{s_L}. \tag{1.4}$$

In the limit of a large ratio of the r.m.s. turbulent velocity v' to the laminar burning velocity s_L the turbulent burning velocity s_T is then proportional to v'

$$s_T \sim v'. \tag{1.5}$$

This simple result has been generalized by Pocheau (1992) who used a renormalization procedure to show that only an expression of the kind

$$\frac{s_T}{s_L} = \left(1 + C\left(\frac{v'}{s_L}\right)^n\right)^{1/n} \tag{1.6}$$

satisfies scale invariance in the corrugated flamelets regime.

For small-scale turbulence Damköhler argued that turbulence modifies the transport between the reaction zone and the unburnt gas. In analogy to the scaling relation for the laminar burning velocity

$$s_L \sim (D/t_c)^{1/2}, \tag{1.7}$$

where t_c is the chemical timescale and D the molecular diffusivity, he used the turbulent diffusivity D_t to obtain

$$s_T \sim \left(D_t/t_c\right)^{1/2}. \tag{1.8}$$

Therefore the ratio

$$\frac{s_T}{s_L} \sim \left(\frac{D_t}{D}\right)^{1/2} \tag{1.9}$$

is independent of t_c, where it is implicitly assumed that the chemical timescale is not affected by turbulence. Since the turbulent diffusivity D_t is proportional to the product $v'\ell$ where ℓ is the integral lengthscale, and the laminar diffusivity is proportional to the product of the laminar burning velocity and the flame thickness ℓ_F one may write (1.9) as

$$\frac{s_T}{s_L} \sim \left(\frac{v'}{s_L}\frac{\ell}{\ell_F}\right)^{1/2} \tag{1.10}$$

showing that for small-scale turbulence the ratio of the turbulent to the laminar burning velocity not only depends on the velocity ratio v'/s_L but also on the lengthscale ratio ℓ/ℓ_F.

In the following half-century there were many attempts to modify Damköhler's analysis and to derive expressions that would reproduce the large amount of experiment data on turbulent burning velocities. Expressions of the form

$$\frac{s_T}{s_L} = 1 + C\left(\frac{v'}{s_L}\right)^n \tag{1.11}$$

have been proposed. The exponent n is often found to be in the vicinity of 0.7 (Williams 1985*a*, p. 429ff.). Attempts to justify a single exponent on the basis of dimensional analysis, however, fall short even of Damköhler's pioneering work; he had recognized the existence of two different regimes in premixed turbulent combustion.

A common feature of all premixed flames seems to be that they contain a chemically inert preheat zone. Recent asymptotic studies for many flames ranging from hydrogen over methane and methanol up to *n*-heptane and *iso*-octane (see Seshadri 1996 for a recent review) have confirmed this classical picture of Zel'dovich & Frank-Kamenetzkii (1938), although the chemical details are quite different (Peters 1997). The chemically inert preheat zone is followed by a thin inner layer in which the fuel is attacked by radicals and is oxidized via chain reactions to CO and H_2. This layer controls the flame structure. It is followed by a post-flame oxidation layer where the final products are formed. The thickness of the inner layer is

$$\ell_\delta = \delta\ell_F, \tag{1.12}$$

where δ is typically of the order 0.1 whereas the preheat zone is of the order of the flame thickness ℓ_F.

In this paper we will consider the case that small eddies of the thickness of the Kolmogorov scale can penetrate into the preheat zone, but not into the inner layer. The reaction zone therefore remains a thin zone, which essentially is not affected by turbulent mixing. We call this the thin reaction zones regime. If the inner layer were disturbed by eddies of its own thickness or smaller, one would expect the entire reaction zone to be disrupted. Thus the chemical timescale is not the same as in laminar flames and Damköhler's assumption leading to (1.9) can no longer be valid. When this happens another regime follows where an interaction between turbulence and chemistry must be considered.

The paper is organized in the following way: In § 2 we will identify the thin reaction zones regime within a regime diagram of premixed turbulent combustion and derive a mixing lengthscale that accounts for the thickening of the preheat zone in that regime. In § 3, as a crucial step of the analysis, we will apply the level-set approach to the thin reaction zone regime and derive an equation for the scalar quantity $G(\boldsymbol{x}, t)$. It is combined with the corresponding G-equation for the corrugated flamelets regime to obtain a formulation that contains the leading-order terms for both regimes. The resulting G-equation is written for non-constant density but does not include gas expansion effects. In § 4 we will derive equations for the Favre average $\widetilde{G}$ and its variance $\widetilde{G''^2}$ for both regimes. Closure of the sink terms in the variance equations leads to scaling relations for the flame surface area ratio $\tilde{\sigma}$ which differs fundamentally in the two regimes. In § 5 we will model a transport equation for $\tilde{\sigma}_t$, the flame surface area ratio increase by turbulence that covers both regimes. Modelling assumptions generally used in two-equation models of turbulence are introduced.

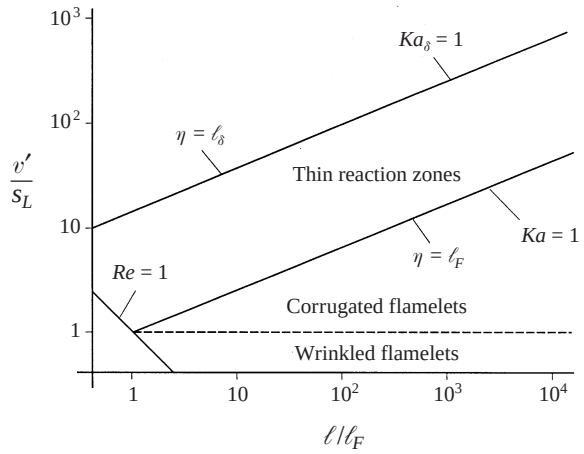

FIGURE 1. Regime diagram for premixed turbulent combustion.

From the balance of the source terms in the $\tilde{\sigma}_t$ equation an algebraic expression for the turbulent burning velocity is then derived. In the Appendix closure relations of the sink terms in the variance equation are derived for the thin reaction zones regime using two-point correlations under the assumption of constant density and isotropic turbulence.

2. Regimes in premixed turbulent combustion

Diagrams defining combustion regimes in terms of length and velocity scale ratios (Borghi 1985; Peters 1986) or in terms of the Reynolds and the Damköhler number (Williams 1985*b*) have been quite popular in recent years. The thin reaction zones regime is shown in a diagram in terms of length and velocity scale ratios in figure 1. One may relate the r.m.s. turbulent velocity v' and the integral turbulent lengthscale ℓ to the turbulent kinetic energy $\bar{k}$ and the dissipation $\bar{\varepsilon}$ as

$$\bar{k} = \tfrac{3}{2}v'^2\,, \quad \bar{\varepsilon} = \frac{v'^3}{\ell} \tag{2.1}$$

and define the integral timescale as

$$\tau = \ell/v'. \tag{2.2}$$

The Kolmogorov length, time and velocity scales are

$$\eta = (\nu^3/\bar{\varepsilon})^{1/4}, \quad t_\eta = (\nu/\bar{\varepsilon})^{1/2}, \quad v_\eta = (\nu\bar{\varepsilon})^{1/4}, \tag{2.3}$$

respectively, where ν is the kinematic viscosity immediately ahead of the inner layer.

For scaling purposes in this section it is useful to set the Schmidt number $\mathrm{Sc} = \nu/D$ equal to unity and to define the flame thickness ℓ_F and the flame time by

$$\ell_F = \frac{D}{s_L} = \frac{\nu}{s_L}\,, \quad t_F = \frac{\ell_F}{s_L}\,. \tag{2.4}$$

Then, as in Peters (1986), we define the turbulent Reynolds number

$$Re = v'\ell/s_L\ell_F, \tag{2.5}$$

and the turbulent Karlovitz number as

$$Ka = t_F/t_\eta = \ell_F^2/\eta^2 = v_\eta^2/s_L^2. \tag{2.6}$$

The different definitions in (2.6) follow from (2.3) and (2.4). Using (1.12) an additional Karlovitz number based on the inner layer thickness ℓ_δ may also be introduced

$$Ka_\delta = \ell_\delta^2/\eta^2 = \delta^2\, Ka. \tag{2.7}$$

The definitions (2.1)–(2.6) can be used to derive the following relations between the ratios v'/s_L and ℓ/ℓ_F in terms of the two non-dimensional numbers Re and Ka as

$$\begin{aligned} v'/s_L &= Re\,(\ell/\ell_F)^{-1} \\ &= Ka^{2/3}(\ell/\ell_F)^{1/3}. \end{aligned} \tag{2.8}$$

In figure 1, the lines $Re = 1$, $Ka = 1$ and $Ka_\delta = 1$ represent boundaries between the different regimes of premixed turbulent combustion. Another boundary of interest is the line $v'/s_L = 1$, which separates the wrinkled and corrugated flamelets. The line $Re = 1$ separates turbulent flames characterized by $Re > 1$ from laminar flames, which are situated in the lower-left corner of the diagram. The remaining three regimes belong to the flamelet regime since they are characterized by the existence of thin layers. The regime of main interest here is the thin reaction zones regime, which is separated by the line $Ka = 1$ from the corrugated flamelets regime. According to (2.6), this is equivalent to the condition that the flame thickness is equal to the Kolmogorov scale (the Klimov–Williams criterion).

The thin reaction zones regime is characterized by $Re > 1$, $Ka > 1$ and $Ka_\delta < 1$, the second inequality indicating that the smallest eddies can enter into the flame structure since $\eta < \ell_F$. The last inequality indicates that eddies of size η are larger than the inner layer thickness ℓ_δ and therefore cannot penetrate into that layer.

According to (2.7), if $\delta = 0.1$ the value $Ka_\delta = 1$ corresponds to $Ka = 100$. This value is used in figure 1 for the upper limit of the thin reaction zones regime. It seems roughly to agree with the flamelet boundary obtained in numerical studies by Poinsot, Veynante & Candel (1991), where two-dimensional interactions between a laminar premixed flame front and a vortex pair were analysed. These simulations correspond to $Ka = 180$ for cases without heat loss and $Ka = 25$ with small heat loss. The former value would correspond to a reaction zone thickness of $\ell_\delta = 0.07\,\ell_F$ and the latter to $\ell_\delta = 0.2\,\ell_F$.

In the thin reaction zones regime small eddies entering into the preheat zone will increase the scalar mixing, therefore destroying the quasi-steady flame structure that exists in the corrugated flamelet regime. Therefore a steady-state burning velocity cannot be defined anymore. But a chemical time, which is of the same order of magnitude as the flame time t_F can still be defined. According to (2.6) the flame time is larger than the Kolmogorov time and therefore lies within the inertial range. This may be used to define a characteristic length scale.

We may define a discrete sequence of eddies within the inertial range by

$$\ell_n = \frac{\ell}{2^n} \geqslant \eta, \quad n = 1, 2, \ldots\ . \tag{2.9}$$

Since the energy transfer $\bar{\varepsilon}$ is constant within the inertial range, dimensional analysis relates the turnover time t_n across the eddy ℓ_n to $\bar{\varepsilon}$ as

$$\bar{\varepsilon} = \frac{\ell_n^2}{t_n^3}. \tag{2.10}$$

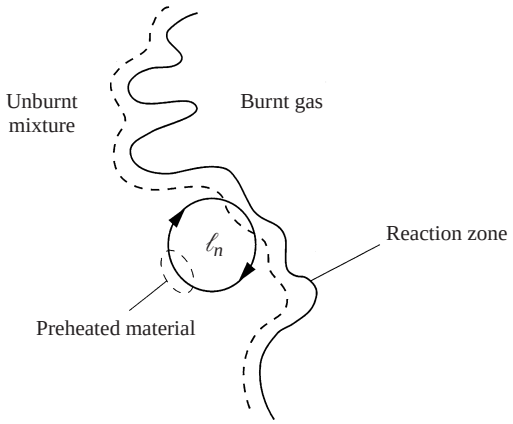

FIGURE 2. Transport of preheated material from a region of thickness ℓ_F by an eddy of size $\ell_n = \ell_m$ during half a turnover time $t_n = t_F$.

If we use (2.4) the flame time may be related to the diffusivity and the flame thickness indicating that it is the time needed for diffusion of heat or chemical species across a distance of the order of ℓ_F

$$t_F = \frac{\ell_F^2}{D}. \tag{2.11}$$

Then, by setting $t_F = t_n$ in (2.10), one obtains the lengthscale

$$\ell_m = (\bar{\varepsilon} t_F^3)^{1/2}. \tag{2.12}$$

This is interpreted as a mixing lengthscale. It was identified by Zimont (1979) and should therefore be called the Zimont scale. It corresponds to the size of an eddy within the inertial range which has a turnover time equal to the time needed to diffuse heat over a distance equal to ℓ_F. During half its turnover time an eddy of size ℓ_m will therefore interact with the advancing reaction front and will be able to transport preheated fluid from a region of thickness ℓ_F in front of the reaction zone over a distance corresponding to its own size. This is schematically shown in figure 2. Much smaller eddies will also do this but since they are smaller, their action will be masked by eddies of size ℓ_m. Much larger eddies have a longer turnover time and would therefore be able to transport structures thicker than ℓ_F across their own size, namely those of thickness between ℓ_F and ℓ_m. They will therefore corrugate the broadened flame structure at scales larger than ℓ_m. The physical interpretation of ℓ_m is that of the maximum distance that preheated fluid will be transported ahead of the reaction zone. The Zimont scale therefore broadens the preheat zone. The regime defined by $\ell_\delta < \eta < \ell_F$ is therefore characterized by thick flames with thin reaction zones.

In a previous paper (Peters 1991) the lengthscale ℓ_m had incorrectly been interpreted as a quench scale ℓ_q. In his thesis Chen (1994) tried to measure ℓ_q by performing simultaneous measurements of temperature as well as of OH and CH concentration fields by using two-dimensional Rayleigh thermometry and laser two-dimensional induced fluorescence in three highly stretched turbulent methane–air Bunsen flames. These flames fall into the thin reaction zones regime. Temperature iso-lines from this thesis are plotted in figure 11 of Chen *et al.* (1996) showing broad regions of elevated temperature in front of the reaction zone. The size of these regions was 1.9, 1.3 and 0.6 mm for the three different flames analysed in Chen (1994), respectively, while the

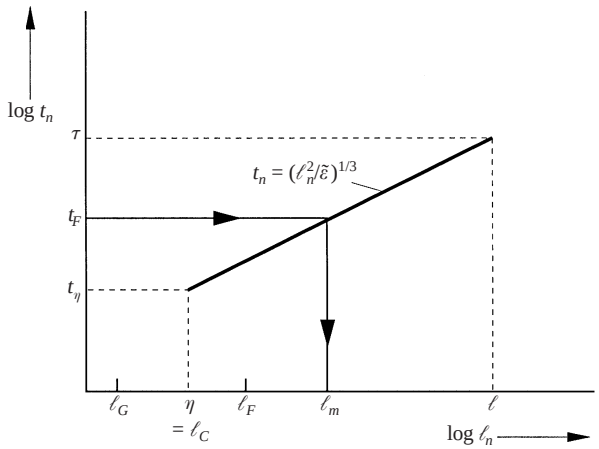

FIGURE 3. Graphical illustration of the mixing scale ℓ_m within the inertial range.

flame thickness ℓ_F was estimated as 0.175 mm. The scale ℓ_q was clearly much larger than the flame thickness.

The derivation of ℓ_m is illustrated in figure 3, showing (2.10) in a log-log plot of t_n over ℓ_n. If one crosses the time axis at $t_F = t_n$, the scale ℓ_m on the lengthscale axis is obtained. If t_F is equal to the Kolmogorov time t_η, figure 3 shows that ℓ_m is equal to the Kolmogorov scale η. In this case, one obtains $\ell_m = \ell_F$ at the border between the thin reaction zones regime and the corrugated flamelets regime. Similarly, if the flame time t_F is equal to the integral time τ, ℓ_m is equal to the integral lengthscale ℓ. This corresponds to the line $Da = 1$ in previous diagrams (Borghi 1985; Peters 1986; Williams 1985*b*). Here, it turns out to have no particular significance in terms of separating regimes of turbulence combustion, but to merely set a limit for the mixing scale ℓ_m which cannot increase beyond the integral scale ℓ. This illustrates that the interaction between turbulence and combustion does not occur at the integral length and timescales.

In figure 3 the flame thickness ℓ_F and the Gibson scale ℓ_G are also shown. The Gibson scale defined by

$$\ell_G = \frac{s_L^3}{\tilde{\varepsilon}} \tag{2.13}$$

(Peters 1986) is smaller than the Kolmogorov scale and has no physical significance in the thin reaction zones regime. The flame thickness ℓ_F is larger than η and smaller than ℓ_m. It may also be noted that, since we have set $\nu = D$, the Kolmogorov length η is equal to the Obukhov–Corrsin scale

$$\ell_C = (D^3/\tilde{\varepsilon})^{1/4}, \tag{2.14}$$

which will be used below.

3. The level-set approach for premixed combustion

It is useful to formulate the problem of premixed combustion in a general flow field in terms of a partial differential equation that does not explicitly contain a chemical source term. Such an equation may be derived for any well-defined front in a flow

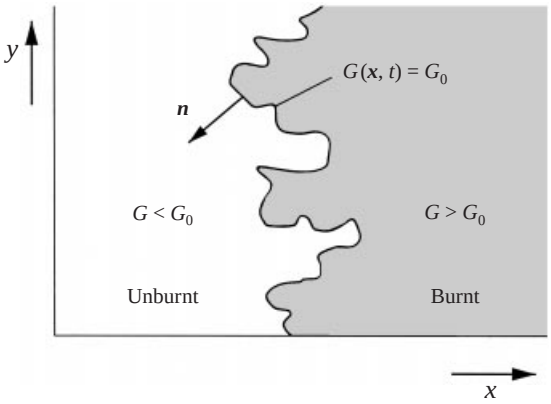

FIGURE 4. A schematic representation of the flame front as an iso-scalar surface of $G(x,t)$.

field by defining the normal vector to the front as

$$\boldsymbol{n} = -\frac{\nabla G}{|\nabla G|} \tag{3.1}$$

and considering an iso-scalar surface representing the front as

$$G(\boldsymbol{x}, t) = G_0, \tag{3.2}$$

where G_0 is arbitrary. If one considers a flame front, the surface $G(\boldsymbol{x},t) = G_0$ divides the flow field into two regions where $G > G_0$ is the region of burnt gas behind the front and $G < G_0$ that in front (figure 4). This is called the level-set approach. Differentiating (3.2) with respect to t one obtains

$$\frac{\partial G}{\partial t} + \nabla G \cdot \frac{\mathrm{d}\boldsymbol{x}}{\mathrm{d}t}\bigg|_{G=G_0} = 0. \tag{3.3}$$

In the corrugated flamelets regime a kinematic balance involving the flow velocity $\boldsymbol{v}$, the burning velocity normal to the front $s_L\boldsymbol{n}$ defines the resulting propagation velocity $\mathrm{d}\boldsymbol{x}/\mathrm{d}t$ of the front as

$$\frac{\mathrm{d}\boldsymbol{x}}{\mathrm{d}t} = \boldsymbol{v} + \boldsymbol{n}\, s_L. \tag{3.4}$$

Introducing (3.4) into (3.5) and multiplying both sides by the density ρ one obtains the equation derived by Williams (1985*b*)

$$\rho \frac{\partial G}{\partial t} + \rho \boldsymbol{v} \cdot \nabla G = \rho s_L |\nabla G| \tag{3.5}$$

which is known as the G-equation in the combustion literature. It contains a local and a convective term but no diffusion term. Instead there is on the right-hand side a propagation term containing the product of the burning velocity s_L and the modulus of G. Since (3.5) was derived at the flame front, it is valid at $G(\boldsymbol{x},t) = G_0$ only. Therefore the density ρ and the velocity $\boldsymbol{v}$ are conditional values at the front. If the flame is assumed to be infinitely thin, the density, the flow velocity and the burning velocity are conveniently defined as those of the unburnt mixture immediately ahead of the flame. Even though the density is constant in the entire unburnt mixture, the flow field immediately ahead of the flame will be influenced by gas expansion due to heat release within the flame front. If, as in the following, the flame is assumed to

be of finite thickness, a location within the flame structure must be defined to assign to $G(\boldsymbol{x}, t)$ the value G_0. Then, the density varies within the flame structure and the velocity field $\boldsymbol{v}$ is affected by density changes.

Although G represents an arbitrary scalar it is convenient to interpret it as the distance from the flame front by imposing the condition $|\nabla G| = 1$ for $G \neq G_0$. Then G has the dimension of a length. It will be called distance function in the following.

The burning velocity s_L in (3.5) may be modified to account for the effect of flame front curvature and flame strain. In asymptotic analyses employing the limit of a large ratio of the fluid dynamic lengthscale to the flame thickness resulting in a quasi-steady structure of the preheat zone, first-order corrections to the burning velocity due to curvature κ and straining of the flame may be derived (Pelce & Clavin 1982; Matalon & Matkowsky 1982) yielding

$$s_L = s_L^0 - s_L^0 \mathscr{L} \kappa + \mathscr{L} \boldsymbol{n} \cdot \nabla \boldsymbol{v} \cdot \boldsymbol{n}. \tag{3.6}$$

Here s_L^0 is the burning velocity of the unstretched flame and $\mathscr{L}$ is the Markstein length.

The flame front curvature κ in (3.6) is defined as

$$\kappa = \nabla \cdot \boldsymbol{n} = \nabla \cdot \left(-\frac{\nabla G}{|\nabla G|} \right) = -\frac{\nabla^2 G - \boldsymbol{n} \cdot \nabla (\boldsymbol{n} \cdot \nabla G)}{|\nabla G|}, \tag{3.7}$$

where $\nabla(|\nabla G|) = -\nabla(\boldsymbol{n} \cdot \nabla G)$ has been used. If (3.6) is introduced into (3.5) the G-equation may be written as

$$\rho \frac{\partial G}{\partial t} + \rho \boldsymbol{v} \cdot \nabla G = \rho s_L^0 \sigma - \rho D_{\mathscr{L}} \kappa \sigma + \rho \mathscr{L} \boldsymbol{n} \cdot \nabla \boldsymbol{v} \cdot \boldsymbol{n} \sigma, \tag{3.8}$$

where $D_{\mathscr{L}} = s_L^0 \mathscr{L}$ is the Markstein diffusivity and

$$\sigma = |\nabla G| \tag{3.9}$$

is the modulus of G conditioned at $G(x, t) = \sigma$. Since the kinematic balance (3.4) is the basis of this equation, we will call it the kinematic G-equation.

The curvature term adds a second-order derivative to the kinematic G-equation. This avoids the formation of cusps and non-unique solutions that would result from (3.5) with a constant value of s_L. The mathematical nature of (3.8) is that of a Hamilton–Jacobi equation with a parabolic second-order differential operator due to the curvature term.

We now want to derive an equivalent level-set formulation for the thin reaction zones regime. Since small eddies enter into the preheat zone of the flame structure we will consider the location immediately ahead of the inner layer as representative for the location of the reaction zone. At that location the deficient reactant (fuel for lean flames or oxygen for rich flames) takes small values. For example, the fuel mass fraction for stoichiometric methane flames, normalized with respect to that in the unburnt mixture, should be of the order of the inner layer thickness δ immediately ahead of the inner layer (Peters 1997). Therefore, for an asymptotically thin inner layer we define the location of the reaction zone by the iso-scalar surface of either the fuel mass fraction Y_F or the oxygen mass fraction Y_{O_2} in the limit $Y_F \to 0$ or $Y_{O_2} \to 0$, respectively. We denote the mass fraction of the deficient species by Y and its iso-scalar value ahead of the inner layer as Y_0 and consider its balance equation

$$\rho \left(\frac{\partial Y}{\partial t} + \boldsymbol{v} \cdot \nabla Y \right) = \nabla \cdot (\rho D \nabla Y) + \dot{m}, \tag{3.10}$$

where D is its diffusion coefficient and $\dot{m}$ its chemical source term. Similarly to (3.3) the iso-scalar surface $Y(\boldsymbol{x},t) = Y_0$ must satisfy the condition

$$\frac{\partial Y}{\partial t} + \nabla Y \cdot \left.\frac{\mathrm{d}\boldsymbol{x}}{\mathrm{d}t}\right|_{Y=Y_0} = 0. \tag{3.11}$$

Gibson (1968) has derived an expression for the displacement speed s_d for an iso-surface of diffusive scalars. Extending this result to a reactive scalar defined by (3.10) (cf. Echekki & Chen 1996) this leads to

$$\left.\frac{\mathrm{d}\boldsymbol{x}}{\mathrm{d}t}\right|_{Y=Y_0} = \boldsymbol{v} + \boldsymbol{n}\, s_d, \tag{3.12}$$

where

$$s_d = \left[\frac{\nabla \cdot (\rho D \nabla Y) + \dot{m}}{\rho |\nabla Y|}\right]_0. \tag{3.13}$$

The normal vector on the iso-concentration surface is defined as

$$\boldsymbol{n} = \left.\frac{\nabla Y}{|\nabla Y|}\right|_{Y=Y_0}. \tag{3.14}$$

We want to formulate a G-equation that describes the location of the thin reaction zones such that the iso-surface $Y(\boldsymbol{x},t) = Y_0$ coincides with the iso-surface defined by $G(\boldsymbol{x},t) = G_0$. Then the normal vector defined by (3.14) is equal to that defined by (3.1) and also points towards the unburnt mixture. Using (3.1) and (3.3) together with (3.13) leads to

$$\rho \frac{\partial G}{\partial t} + \rho \boldsymbol{v} \cdot \nabla G = -\left[\frac{\nabla \cdot (\rho D \nabla Y) + \dot{m}}{|\nabla Y|}\right]_0 |\nabla G|. \tag{3.15}$$

Echekki & Chen (1998) show that the diffusive term appearing on the right-hand side of (3.15) may be split into one term accounting for curvature and another for diffusion normal to the iso-surface

$$\nabla \cdot (\rho D \nabla Y) = \rho D |\nabla Y| \nabla \cdot \boldsymbol{n} + \boldsymbol{n} \cdot \nabla (\rho D \boldsymbol{n} \cdot \nabla Y), \tag{3.16}$$

where the definition (3.14) has been used. This is consistent with the definition (3.7) if (3.1) is replaced by (3.14). When (3.16) is introduced into (3.15) it can be written as

$$\rho \frac{\partial G}{\partial t} + \rho \boldsymbol{v} \cdot \nabla G = -\rho D\, \kappa |\nabla G| + \rho\, (s_n + s_r) |\nabla G|. \tag{3.17}$$

Here κ may be expressed by (3.7) in terms of the G-field. The quantities s_n and s_r are contributions due to normal diffusion and reaction to the displacement speed of the thin reaction zone and are defined as

$$\rho s_n = -\frac{\boldsymbol{n} \cdot \nabla (\rho D \boldsymbol{n} \cdot \nabla Y)}{|\nabla Y|}, \tag{3.18}$$

$$\rho s_r = -\frac{\dot{m}}{|\nabla Y|}. \tag{3.19}$$

In a steady, unstretched planar laminar flame the sum of ρs_n and ρs_r would be equal to the mass flow rate ρs_L^0. Here, however, the unsteady mixing and diffusion of all chemical species and the temperature in the regions ahead of the thin reaction zone will influence the local displacement speed. Therefore the sum of s_n and s_r cannot be prescribed, but is a fluctuating quantity, that couples the G-equation to the solution of

the balance equations of the reactive scalars. There is reason to expect, however, that the sum of the values of s_n and s_r, defined by $s_L^\star$, is of the same order of magnitude as the laminar burning velocity s_L^0. A recent evaluation of DNS-data (Peters *et al.* 1998) confirms that estimate. In that paper it is also found that the mean values of s_n and s_r depend slightly on curvature. This leads to a modification of the diffusion coefficient D which takes Markstein effects into account. We will ignore these modifications here and consider the following model equation for the thin reaction zone regime:

$$\rho \frac{\partial G}{\partial t} + \rho \boldsymbol{v} \cdot \nabla G = -\rho D \kappa \sigma + \rho s_L^* \sigma \tag{3.20}$$

where (3.9) has been used. This equation, valid in the thin reaction zones regime, will be called the diffusive G-equation. It is very similar to the kinematic G-equation (3.8), which was derived for the corrugated flamelets regime. An important difference, apart from the difference between s_L^0 and s_L^*, is the difference between $D_{\mathscr{D}}$ and D and the disappearance of the strain term in (3.20) as compared to (3.8). The Markstein diffusivity $D_{\mathscr{D}}$, although of the same order of magnitude as D, may even be negative if, as for lean hydrogen flames, the Lewis number is sufficiently smaller than unity. Then the kinematic G-equation is ill-posed and must be modified to be able to describe thermo-diffusive instabilities as analysed by Sivashinsky (1977). The diffusive G-equation does not pose such problems since D is always positive.

In an analytical study of the response of one-dimensional constant-density flames to time-dependent stretch and curvature, Joulin (1994) has shown that in the limit of high-frequency perturbations the effect of strain disappears entirely and Lewis-number effects also disappear in the curvature term such that $D_{\mathscr{D}}$ approaches D. This analysis was based on one-step large-activation-energy asymptotics with the assumption of a single thin reaction zone. It suggests that (3.20) could also have been derived from (3.8) for the limit of high-frequency perturbations of the flame structure. This strongly supports the physical picture derived for the thin reaction zones regime.

It is interesting to analyse the order of magnitude of the different terms in (3.20) for conditions where Kolmogorov eddies enter into the preheat zone. This can be done by normalizing the independent quantities and the curvature in this equation with respect to Kolmogorov length and timescales

$$\hat{t} = t/t_\eta, \ \hat{\boldsymbol{x}} = \boldsymbol{x}/\eta, \quad \hat{\kappa} = \eta\kappa, \ \hat{\nabla} = \eta\nabla. \tag{3.21}$$

Using $\eta^2/t_\eta = \nu$ one obtains

$$\frac{\partial G}{\partial \hat{t}} + \frac{\boldsymbol{v} \cdot \hat{\nabla} G}{v_\eta} = -\frac{D}{\nu}\hat{\kappa}|\hat{\nabla} G| + \frac{s_L^*}{v_\eta}|\hat{\nabla} G| \,. \tag{3.22}$$

Since Kolmogorov eddies can perturb the flow field that acts on the G-field, all derivatives, the curvature and the velocity ratio $\boldsymbol{v}/v_\eta$ are typically of order unity. In flames D/ν is also of order unity. However, in the thin reaction zones regime the Karlovitz number is larger than unity and thereby, due to (2.6)

$$v_\eta > s_L^*, \tag{3.23}$$

indicating that the last term in (3.22) will be small and on the right-hand side the first term containing the curvature will be dominant. This indicates that wrinkling of the reaction zone front by small eddies, leading to large local curvatures, is responsible for the advancement of the front. Applying the same order of magnitude analyses to (3.8) shows that in the corrugated flamelets regime, since the Karlowitz number is

smaller than unity, the propagation term $s_L^0\sigma$ is dominant and the effect of curvature and strain are of lower order.

We want to base the following analysis on an equation which contains only the leading-order terms in both regimes. Therefore we keep the propagation term $s_L^0\sigma$ and the strain term $\mathscr{L}\boldsymbol{n}\cdot\nabla\boldsymbol{v}\cdot\boldsymbol{n}\sigma$ in (3.8) from the corrugated flamelets regime and the curvature term $D\,\kappa\sigma$ in (3.20) from the thin reaction zones regime. The leading-order equation valid in both regimes then is

$$\rho\frac{\partial G}{\partial t}+\rho\boldsymbol{v}\cdot\nabla G=\rho s_L^0\sigma-\rho D\,\kappa\sigma+\rho\mathscr{L}\boldsymbol{n}\cdot\nabla\boldsymbol{v}\cdot\boldsymbol{n}\sigma. \tag{3.24}$$

4. Modelling premixed turbulent combustion for both regimes

The important step in applying the G-equation either in numerical simulations or for turbulence modelling is to assume its validity not only at $G(\boldsymbol{x},t)=G_0$ but in the entire flow field. Then the G-equation has properties of a field equation. These properties have been investigated for turbulent flow fields in a number of papers. In particular Kerstein, Ashurst & Williams (1988) have performed direct numerical simulations in a cubic box assuming constant density throughout such that the flow field was not affected by the flame. Then all G-levels could be interpreted as representing a flame front. They therefore could consider G_0 as a variable and average over all values of G_0 to show that for large times the mean modulus of G may be interpreted as the flame surface area ratio F_T/F, which according to (1.2) is equal to the ratio of the turbulent to the laminar burning velocity

$$\bar{\sigma}=\overline{|\nabla G|}=\frac{s_T}{s_L}. \tag{4.1}$$

A similar approach has recently been used by Ulitsky & Collins (1997) to determine the effect of large coherent structures on the turbulent burning velocity.

Peters (1992) considered turbulent modelling of the kinematic G-equation and derived Reynolds-averaged equations for the mean $\overline{G}$ and the variance $\overline{G'^2}$. A constant density was assumed and G and the velocity component v_α were split into a mean and a fluctuation. The main source term in the variance equation resulted from the propagation term $s_L^0\sigma$ in (3.8) and was defined as

$$\overline{\omega}=-2\,s_L^0\,\overline{\sigma G'}. \tag{4.2}$$

This term was called kinematic restoration in order to emphasize the kinematic effect of local laminar flame propagation. It accounts for the smoothing effect of the G-field and thereby the flame surface by flame advancement with the laminar burning velocity. Flame front corrugations produced by turbulence are restored by this kinematic effect. Closure of this term was achieved by deriving a scalar spectrum function for two-point correlations of G in the limit of a large ratio of v'/s_L^0 and large Reynolds numbers. From the analysis an expression results which relates $\overline{\omega}$ to the variance $\overline{G'^2}$ and $\tilde{k}/\tilde{\varepsilon}$ as

$$\overline{\omega}=c_\omega\,\frac{\tilde{\varepsilon}}{\tilde{k}}\,\overline{G'^2} \tag{4.3}$$

with $c_\omega=1.62$. This expression shows that kinematic restoration plays a similar role for fluctuations of the flame front as scalar dissipation plays for fluctuations of diffusive scalars.

It was also shown that kinematic restoration is active at the Gibson scale, since ℓ_G represents the first cut-off from the inertial range in the scalar spectrum function and

therefore is responsible for removing scalar fluctuations. A dissipation term involving the Markstein diffusivity was shown to be most effective at the Obukhov–Corrsin scale ℓ_C and a term called scalar-strain co-variance was shown to be most effective at the Markstein length $\mathscr{L}$. In the corrugated flamelets regime the Gibson scale is larger than ℓ_C and $\mathscr{L}$. Therefore these additional terms can be neglected.

The scaling relation (4.3) shows that in the limits of large ratios v'/s_L^0 and large Reynolds numbers the kinematic restoration is independent of s_L^0 and can be modelled in terms of quantities defined at the integral scales. Thereby the variance equation becomes independent of s_L^0. This also suggests that the mean propagation term $s_L^0\bar{\sigma}$ should be independent of s_L^0 in this limit. Dimensional analysis then suggests the scaling relations

$$s_L^0\bar{\sigma} \sim \left(\frac{\bar{\varepsilon}}{\bar{k}}\overline{\omega}\right)^{1/2} \sim \frac{\bar{\varepsilon}}{\bar{k}}(\overline{G'^2})^{1/2}. \tag{4.4}$$

For steady-state turbulent flames the variance $\overline{G'^2}$ was shown to be proportional to the square of the integral lengthscale ℓ (cf. (5.21 below)). Using (2.1) and (4.1) one obtains

$$s_T \sim v',$$

which is Damköhler's result (1.5) for the turbulent burning velocity in the large-scale turbulence limit. We note that it is valid for the corrugated flamelets regime only.

A similar analysis as in Peters (1992) can be performed for both regimes based on (3.24). If this equation is considered to be valid everywhere in the flow field, the effect of variable density may be included by considering Favre averages by splitting G and the velocity component into Favre means and fluctuations

$$G = \widetilde{G} + G'', \quad v_\alpha = \tilde{v}_\alpha + v''_\alpha. \tag{4.5}$$

This leads to an equation for the Favre mean value of G

$$\overline{\rho}\frac{\partial\widetilde{G}}{\partial t} + \overline{\rho}\,\tilde{\boldsymbol{v}}\cdot\nabla\widetilde{G} + \nabla(\overline{\rho}\,\widetilde{\boldsymbol{v}''G''}) = -\overline{\rho}D\,\widetilde{\kappa\sigma} + \overline{\rho}\,s_L^0\tilde{\sigma} + \overline{\rho}\,\widetilde{\mathscr{L}\boldsymbol{n}\cdot\nabla\boldsymbol{v}\cdot\boldsymbol{n}\sigma}. \tag{4.6}$$

The condition $\widetilde{G} = G_0$ now defines the location of the mean flame front, while the Favre variance $\widetilde{G''^2}$ accounts for flame front fluctuations and thereby is a measure of the flame brush thickness. We will not enter into the modelling of the different terms in (4.6) in this paper except for the quantity $\tilde{\sigma}$ in the propagation term, for which an equation will be derived in § 5. Models for the other terms are discussed in Bray & Peters (1994).

The equation for $\widetilde{G''^2}$ may be derived by subtracting (4.6) from (3.24) to obtain an equation for G''. After multiplying this by $2G''$ and averaging one obtains

$$\overline{\rho}\frac{\partial\widetilde{G''^2}}{\partial t} + \overline{\rho}\,\tilde{\boldsymbol{v}}\cdot\nabla\widetilde{G''^2} + \nabla\cdot(\overline{\rho}\,\widetilde{\boldsymbol{v}''G''^2}) = -2\overline{\rho}\,\widetilde{\boldsymbol{v}''G''}\cdot\nabla\widetilde{G} - \overline{\rho}\tilde{\omega} - \overline{\rho}\tilde{\chi} - \overline{\rho}D\widetilde{\mathscr{K}\sigma}. \tag{4.7}$$

Here the derivation of the terms on the left-hand side and the first term on the right-hand side is straightforward. The Favre kinematic restoration $\tilde{\omega}$ is important in the corrugated flamelets regime only (see the Appendix) and is defined similarly to (4.2). The scalar-strain co-variance was neglected because it is small in the corrugated flamelets regime as shown in Peters (1992) and does not appear in the thin reaction zones regime. The last two terms represent scalar dissipation $\tilde{\chi}$ and a curvature term $\widetilde{\mathscr{K}\sigma}$. They originate from the second term on the right-hand side of (3.24) which,

multiplied with $2G''$, leads after averaging to a term of the form

$$-2\bar{\rho}D\widetilde{G''\kappa\sigma}.$$

In order to interpret this term we split the product $G''\kappa\sigma$ into two terms

$$2\,G''\kappa\sigma = -\nabla\cdot\left(2\frac{G''\nabla G}{|\nabla G|}\right)|\nabla G| + 2\nabla G''\nabla G. \tag{4.8}$$

After averaging one may replace products like $\widetilde{G\,G''}$ and $\nabla\widetilde{G''\nabla G}$ by $\widetilde{G''^2}$ and $\nabla\widetilde{G''\nabla G''}$, respectively, to obtain

$$-2\bar{\rho}D\widetilde{G''\kappa\sigma} = -\bar{\rho}D\widetilde{\mathscr{K}\sigma} - \bar{\rho}\tilde{\chi}, \tag{4.9}$$

where $\mathscr{K}$ is a curvature-like term defined by

$$\mathscr{K} = \nabla\cdot\left(-\frac{\nabla G''^2}{|\nabla G|}\right) \tag{4.10}$$

and

$$\tilde{\chi} = 2D(\widetilde{\nabla G''})^2 \tag{4.11}$$

is the scalar dissipation defined in the usual way.

Closure of the sink terms $\tilde{\omega}$ and $\tilde{\chi}$ in (4.7) proceeds in a similar way as in Peters (1992) and is shown in the Appendix. However, owing to the order of magnitude analysis performed in § 3, the dominant term in the thin reaction zones regime is the scalar dissipation term rather than the kinematic restoration term. The closure relation for the scalar dissipation is then obtained as

$$\widetilde{\chi} = c_\chi\frac{\tilde{\varepsilon}}{\tilde{k}}\widetilde{G''^2}, \tag{4.12}$$

where $c_\chi = 1.62$. This closure is standard (Jones 1994) and shows that $\tilde{\chi}$ becomes independent of the molecular diffusivity in the limit of large Reynolds numbers. Therefore, since $\tilde{\omega}$ is small and the last term in (4.7) can be neglected in that limit, the solution of the variance equation becomes independent of D.

However, as in the corrugated flamelet regime, we need to find the appropriate scaling relation for $\tilde{\sigma}$. Introducing an artificial dimension for the distance function G, say g, one finds that $\tilde{\chi}$ has the dimension $\mathrm{g}^2\,\mathrm{s}^{-1}$ and $\tilde{\sigma}$ has the dimension $\mathrm{g\,m}^{-1}$. Dimensional analysis for the thin reaction zone regime must involve the molecular diffusivity D rather than the burning velocity, since the curvature term in (3.20) was found to be dominant. For large Reynolds numbers one therefore obtains the scaling

$$\tilde{\chi} \sim D\tilde{\sigma}^2 \sim \frac{\tilde{\varepsilon}}{\tilde{k}}\widetilde{G''^2}. \tag{4.13}$$

With (2.1) the ratio $\tilde{\varepsilon}/\tilde{k}$ can be expressed in terms of D_t/ℓ^2 since $D_t \sim v'\ell$. Again, since the variance $\widetilde{G''^2}$ is proportional to the square of the integral lengthscale for steady-state turbulent flames this scaling relation for $\tilde{\sigma}$ can be used with (4.1) to derive a relation for the turbulent burning velocity

$$\frac{s_T}{s_L} \sim \left(\frac{D_t}{D}\right)^{1/2},$$

which is Damköhler's expression (1.9) for small-scale turbulence.

This surprising result for the turbulent burning velocity needs a further physical interpretation. As noted in the introduction, Damköhler had simply used the scaling

for the laminar burning velocity and had replaced the molecular diffusivity by the turbulent diffusivity. Here the scaling arguments are quite different. In the thin reaction zones regime turbulent eddies can enter into the chemically inert preheat zone and increase the mixing process. This is accounted for in (4.12) based on spectral scalar transfer between the integral scale and the Kolmogorov scale by relating $\tilde{\chi}$ defined by (4.11) to quantities defined at the integral scales. This requires that scalar mixing down to the Kolmogorov scale occurs immediately ahead of the inner layer. In order to understand the meaning of $\tilde{\sigma}$ in the thin reaction zones regime we define a Taylor lengthscale λ_G of the diffusive G-equation by

$$\tilde{\chi} \sim D\frac{\widetilde{G''^2}}{\lambda_G^2} = D\tilde{\sigma}^2 \quad \text{or} \quad \tilde{\sigma} = \frac{(\widetilde{G''^2})^{1/2}}{\lambda_G}. \tag{4.14}$$

Then, using (2.3) for the Kolmogorov time with $\nu = D$, (2.1) and (4.13) result in

$$\lambda_G \sim v' t_\eta. \tag{4.15}$$

This shows that the Taylor scale λ_G may be interpreted as the distance over which an integral eddy with turnover velocity v' will transport a Kolmogorov eddy during its own turnover time. Since during that time concentrations and temperature fully diffuse across a Kolmogorov eddy the scale λ_G represents the distance necessary for molecular mixing.

Since $\tilde{\sigma}$ was interpreted according to (4.1) as the flame surface area ratio, and $\widetilde{G''^2}$ is proportional to the square of the flame brush thickness, (4.14) shows how much the flame surface area ratio must increase in order to obtain molecular mixing immediately ahead of the inner layer. Equation (4.14) may also be written as

$$\lambda_G F_T = (\widetilde{G''^2})^{1/2} F. \tag{4.16}$$

Similar to the interpretation given in Bray & Peters (1994) for the corrugated flamelets regime, this geometrical relation illustrates for the thin reaction zones regime that λ_G may be interpreted as a lengthscale of flame crossings within the turbulent flame brush.

5. A model equation for the flame surface area ratio for both regimes

In this section we want to derive a model equation for the flame surface area ratio that is valid in both the corrugated flamelets regime and the thin reaction zones regime. For thin flames in a constant-density flow the quantity $\bar{\sigma} = \overline{|\nabla G|}$ was interpreted according to (4.1) as the flame surface area ratio. For illustration purposes we will therefore first derive an equation for σ by dividing (3.24) by the local density ρ and apply the ∇-operator to both sides. Multiplying this with $-\boldsymbol{n} = \nabla G/|\nabla G|$ one obtains

$$\frac{\partial \sigma}{\partial t} + \boldsymbol{v} \cdot \nabla \sigma = -\boldsymbol{n} \cdot \nabla \boldsymbol{v} \cdot \boldsymbol{n} \sigma + s_L^0(\kappa\sigma + \nabla^2 G) - D[\nabla \cdot (\kappa \nabla G) + \kappa^2 \sigma]. \tag{5.1}$$

Here the terms proportional to D are a result of the transformation

$$\boldsymbol{n} \cdot \nabla(\kappa\sigma) = -\nabla G \cdot \nabla \kappa - \kappa \nabla^2 G - \kappa^2 \sigma = -\nabla \cdot (\kappa \nabla G) - \kappa^2 \sigma. \tag{5.2}$$

The first term on the right-hand side of (5.1) accounts for straining by the flow field. It will lead to an increase of flame surface area ratio. The second term containing the laminar burning velocity will have the same effect as kinematic restoration has in the

variance equation. The last term is proportional to D and its effect will be similar to that of scalar dissipation on the variance.

Since closure of (5.1) cannot be derived in a systematic way we revert to the scaling relations (4.4) and (4.13) which relate $\tilde{\sigma}$ to $\tilde{\varepsilon}/\tilde{k}$ and $\widetilde{G''^2}$. However, since these relations were derived for the limit of large v'/s_L^0 and large Reynolds numbers only, they account only for the increase of the flame surface area ratio due to turbulence, beyond the laminar value $\tilde{\sigma} = 1$ for $v' \to 0$. We will therefore write $\tilde{\sigma}$ as

$$\tilde{\sigma} = 1 + \tilde{\sigma}_t \tag{5.3}$$

where $\tilde{\sigma}_t$ is the contribution of turbulence to the flame surface area ratio $\tilde{\sigma}$.

In the following we place ourselves in the context of two-equation modelling and use the algebraic scaling relations (4.4) and (4.13) in order to combine (4.7) for $\widetilde{G''^2}$ with equations for the Favre-averaged turbulent kinetic energy $\tilde{k}$ and the dissipation $\tilde{\varepsilon}$. Since we intend to derive an algebraic equation for the turbulent burning velocity we do not need and will not present models for turbulent transport terms. Therefore we do not explicitly consider the last term on the left-hand side of (4.7). We also neglect the last term on the right-hand side of (4.7) since it is small in the large Reynolds number limit. In addition, we use the closure relation for the sum of $\tilde{\omega} + \tilde{\chi}$ from (A 28) in the Appendix and write (4.7) as

$$\rho \frac{\partial \widetilde{G''^2}}{\partial t} + \bar{\rho}\tilde{\boldsymbol{v}} \nabla \widetilde{G''^2} = -2\bar{\rho}\widetilde{\boldsymbol{v}''G''} \cdot \nabla \widetilde{G} - c_s \bar{\rho} \frac{\tilde{\varepsilon}}{\tilde{k}} \widetilde{G''^2} + (\text{turbulent transport terms}). \tag{5.4}$$

The equations for $\tilde{k}$ and $\tilde{\varepsilon}$ are written as

$$\bar{\rho}\frac{\partial \tilde{k}}{\partial t} + \bar{\rho}\tilde{\boldsymbol{v}} \cdot \nabla \tilde{k} = \bar{\rho}\left(-\widetilde{v'_\alpha v'_\beta}\right)\frac{\partial \widetilde{v}_\alpha}{\partial x_\beta} - \bar{\rho}\,\tilde{\varepsilon} + (\text{turbulent transport terms}), \tag{5.5}$$

$$\bar{\rho}\frac{\partial \tilde{\varepsilon}}{\partial t} + \bar{\rho}\,\tilde{\boldsymbol{v}} \cdot \nabla \tilde{\varepsilon} = c_{\varepsilon 1}\frac{\tilde{\varepsilon}}{\tilde{k}}\left(-\widetilde{v'_\alpha v'_\beta}\right)\frac{\partial \widetilde{v}_\alpha}{\partial x_\beta} - c_{\varepsilon 2}\frac{\tilde{\varepsilon}^2}{\tilde{k}} + (\text{turbulent transport terms}), \tag{5.6}$$

with $c_{\varepsilon 1} = 1.44$ and $c_{\varepsilon 2} = 1.92$. We interpret (4.4) and (4.13) to be relations between $\tilde{\sigma}_t$, $\tilde{\varepsilon}/\tilde{k}$ and $\widetilde{G''^2}$ and we are now able to derive model equations for $\tilde{\sigma}_t$ in the two regimes. We will start with the corrugated flamelets regime and will use (4.4) to derive a differential relation between $\tilde{\sigma}_t$ and $\tilde{\varepsilon}$, $\tilde{k}$ and $\widetilde{G''^2}$ as

$$\frac{\mathrm{d}\tilde{\sigma}_t}{\tilde{\sigma}_t} = \frac{\mathrm{d}\tilde{\varepsilon}}{\tilde{\varepsilon}} - \frac{\mathrm{d}\tilde{k}}{\tilde{k}} + \frac{1}{2}\frac{\mathrm{d}\widetilde{G''^2}}{\widetilde{G''^2}}. \tag{5.7}$$

Combining (5.3)–(5.6) one obtains an equation for $\tilde{\sigma}_t$ of the form

$$\begin{aligned}\bar{\rho}\frac{\partial \tilde{\sigma}_t}{\partial t} + \bar{\rho}\tilde{\boldsymbol{v}} \cdot \nabla \tilde{\sigma}_t = (c_{\varepsilon 1} - 1)\bar{\rho}\frac{(-\widetilde{v''_\alpha v''_\beta})}{\tilde{k}}\frac{\partial \widetilde{v}_\alpha}{\partial x_\beta}\tilde{\sigma}_t + \bar{\rho}\frac{(-\widetilde{\boldsymbol{v}''G''}) \cdot \nabla \widetilde{G}}{\widetilde{G''^2}}\tilde{\sigma}_t \\ - \left(c_{\varepsilon 2} - 1 + \frac{c_s}{2}\right)\bar{\rho}\frac{\tilde{\varepsilon}}{\tilde{k}}\tilde{\sigma}_t + (\text{turbulent transport terms}).\end{aligned} \tag{5.8}$$

In this equation the terms on the left-hand side represent the unsteady change and convection of $\tilde{\sigma}_t$. The first term represents the production of the flame surface area ratio by mean velocity gradients and the second term that by local turbulent fluctuations. The last term accounts for the destruction of the flame surface area ratio by kinematic restoration. It may be cast into a form proportional to s_L^0 by replacing

$\tilde{\varepsilon}/\tilde{k}$ using (4.4) as

$$\frac{\tilde{\varepsilon}}{\tilde{k}} \sim s_L^0 \frac{\tilde{\sigma}_t}{(\widetilde{G''^2})^{1/2}}. \tag{5.9}$$

In the corrugated flamelets regime the model equation for the increase of the flame surface area ratio due to turbulence is then

$$\bar{\rho}\frac{\partial \tilde{\sigma}_t}{\partial t} + \bar{\rho}\tilde{\boldsymbol{v}} \cdot \nabla \tilde{\sigma}_t = c_0 \bar{\rho} \frac{(\widetilde{-v_\alpha'' v_\beta''})}{\tilde{k}} \frac{\partial \tilde{v}_\alpha}{\partial x_\beta} \tilde{\sigma}_t + \bar{\rho} \frac{D_t (\nabla \widetilde{G})^2}{\widetilde{G''^2}} \tilde{\sigma}_t$$
$$- c_2 \bar{\rho} \frac{s_L^0 \tilde{\sigma}_t^2}{(\widetilde{G''^2})^{1/2}} + (\text{turbulent transport terms}) \tag{5.10}$$

where $c_0 = c_{\varepsilon 1} - 1 = 0.44$. The last term contains the constant c_2 which needs to be determined by comparison with experiments. In the turbulent production term we have used the gradient flux approximation

$$(\widetilde{-\boldsymbol{v}'' G''}) = D_t \nabla \widetilde{G}. \tag{5.11}$$

It may be used here but as shown in Bray & Peters (1994) this modelling assumption should not be introduced into (4.6) because there it would result in an elliptic term which contradicts the parabolic character of the G-equation.

Differently from the usual model equations that are valid in the large Reynolds number limit like those for $\tilde{k}$ and $\tilde{\varepsilon}$ (5.10) contains a molecular quantity, the laminar burning velocity. Therefore $\tilde{\sigma}_t$ cannot be defined at the integral scales, but as noted at the end of § 4, it is inversely proportional to the Taylor length λ_G. However, if (5.10) is multiplied with s_L^0, one obtains an equation for the product $s_L^0 \tilde{\sigma}_t$, which according to (4.4) is a quantity defined at the integral scales.

A similar approach can be taken in the thin reaction zones regime where now the scalar dissipation $\tilde{\chi}$ is the main term responsible for reducing fluctuations of the reaction zone. Using (4.13) this leads to the differential relation

$$2\frac{\mathrm{d}\tilde{\sigma}_t}{\tilde{\sigma}_t} = \frac{\mathrm{d}\tilde{\varepsilon}}{\tilde{\varepsilon}} - \frac{\mathrm{d}\tilde{k}}{\tilde{k}} + \frac{\mathrm{d}\widetilde{G''^2}}{\widetilde{G''^2}} \tag{5.12}$$

rather than (5.7). We then obtain an equation similar to (5.10), except with a factor 2 in front of the turbulent production term and c_s replacing $c_s/2$ in the last term. In the last term, however, we now use (4.13) to replace $\tilde{\varepsilon}/\tilde{k}$ as

$$\frac{\tilde{\varepsilon}}{\tilde{k}} \sim \frac{D\tilde{\sigma}_t^2}{\widetilde{G''^2}}. \tag{5.13}$$

Therefore, in the thin reaction zones regime the following equation is obtained:

$$\bar{\rho}\frac{\partial \tilde{\sigma}_t}{\partial t} + \bar{\rho}\tilde{\boldsymbol{v}} \cdot \nabla \tilde{\sigma}_t = c_0 \bar{\rho} \frac{(\widetilde{-v_\alpha'' v_\beta''})}{\tilde{k}} \frac{\partial \tilde{v}_\alpha}{\partial x_\beta} \tilde{\sigma}_t + 2\,\bar{\rho} \frac{D_t (\nabla \widetilde{G})^2}{\widetilde{G''^2}} \tilde{\sigma}_t$$
$$- c_3 \bar{\rho} \frac{D\tilde{\sigma}_t^3}{\widetilde{G''^2}} + (\text{turbulent transport terms}). \tag{5.14}$$

The last term in (5.14) contains the constant c_3 which must be determined empirically. It is proportional to $\tilde{\sigma}_t^3$ and therefore differs from the last term in (5.10) which was proportional to $\tilde{\sigma}_t^2$. It models the effect of scalar dissipation on the flame surface area increase and displays the fundamental difference between the two regimes. Equation (5.14) contains a molecular quantity, the diffusivity D. As for (5.10) we conclude

that $\tilde{\sigma}_t$ cannot be a quantity defined at the integral scales. However, if we multiply (5.14) with $D\tilde{\sigma}_t$, we obtain an equation for $D\tilde{\sigma}_t^2$, which is again a quantity defined at the integral scales according to (4.13). This also justifies the appearance of a term proportional to $\tilde{\sigma}_t^3$ in (5.14).

At this point we take guidance from (5.1) which, after averaging, contains sink terms proportional to s_L^0 and to D. Therefore the last terms in (5.10) and (5.14) are assumed to be additive, the former accounting for flame surface area ratio destruction in the corrugated flamelets regime and the latter that in the thin reaction zones regime. A model equation for $\tilde{\sigma}_t$ that covers both regimes would therefore be

$$\bar{\rho}\frac{\partial\tilde{\sigma}_t}{\partial t}+\bar{\rho}\tilde{\boldsymbol{v}}\cdot\nabla\tilde{\sigma}_t=c_0\bar{\rho}\frac{(-\widetilde{v_\alpha''v_\beta''})}{\tilde{k}}\frac{\partial\widetilde{u_\alpha}}{\partial x_\beta}\tilde{\sigma}_t+c_1\bar{\rho}\frac{D_t(\nabla\widetilde{G})^2}{\widetilde{G''^2}}\tilde{\sigma}_t$$
$$-c_2\bar{\rho}\frac{s_L^0\tilde{\sigma}_t^2}{(\widetilde{G''^2})^{1/2}}-c_3\bar{\rho}\frac{D\tilde{\sigma}_t^3}{\widetilde{G''^2}}+(\text{turbulent transport terms}). \quad (5.15)$$

The last three terms in this equation represent the turbulent production, the kinematic restoration and the scalar dissipation of the flame surface area ratio, respectively, and correspond to the three terms on the right-hand side of (5.1). A constant c_1 has been introduced for a model of the production term that would be valid in both regimes.

We now want to fix the constants c_1, c_2 and c_3 in (5.15) at least tentatively. Existing data and burning velocity data by Abdel-Gayed & Bradley (1981) and Bradley (1992) provide some guidance that we will use. For simplicity we will consider the case of isotropic fully developed turbulence and a fully developed steady-state turbulent flame. In that limit the production term in (5.4) balances the sink term and one obtains with (5.11)

$$2\,D_t(\nabla\widetilde{G})^2=c_s\frac{\tilde{\varepsilon}}{\tilde{k}}\widetilde{G''^2}. \quad (5.16)$$

As for the instantaneous G-equation we will also impose $|\nabla\widetilde{G}|=1$ for $\widetilde{G}\neq G_0$. This can be achieved numerically by a procedure called re-initialization (Sussman, Fatemi & Osher 1994). As a consequence we set $|\nabla\widetilde{G}|=1$ in (5.16). Furthermore, we relate the integral lengthscale to v' and $\tilde{\varepsilon}$ as in Bray (1990)

$$\ell=0.37\,v'^3/\tilde{\varepsilon}, \quad (5.17)$$

use a turbulent Schmidt number of $Sc_t=\nu_t/D_t=0.7$ and the model for the eddy viscosity

$$\nu_t=0.09\frac{\tilde{k}^2}{\tilde{\varepsilon}} \quad (5.18)$$

to obtain for the turbulent diffusivity the expression

$$D_t=0.78\,v'\ell. \quad (5.19)$$

For $\tilde{\varepsilon}/\tilde{k}$ we obtain with (2.1) the relation

$$\frac{\tilde{\varepsilon}}{\tilde{k}}=0.247\frac{v'}{\ell}. \quad (5.20)$$

Taking $c_s=2.0$ from the Appendix (5.16) provides the following estimate for the flame brush thickness:

$$\ell_{F,t}=(\widetilde{G''^2})^{1/2}=c_4\,\ell \quad (5.21)$$

where $c_4=1.78$.

Similarly to (5.16) the balance of turbulent production, kinematic restoration and scalar dissipation in (5.15) leads with $|\nabla\widetilde{G}| = 1$ and (5.21) to

$$c_1 \frac{D_t}{\ell_{F,t}^2}\tilde{\sigma}_t - c_2 \frac{s_L^0}{\ell_{F,t}}\tilde{\sigma}_t^2 - c_3 \frac{D}{\ell_{F,t}^2}\tilde{\sigma}_t^3 = 0. \tag{5.22}$$

This equation covers two limits: in the corrugated flamelets regime the first two terms should balance while in the thin reaction zones regime we have the balance of the first and the last term. With (5.19) and (5.21) it follows for the corrugated flamelet regime that

$$c_2\, c_4\, s_L^0 \tilde{\sigma}_t = 0.78\, c_1 v'. \tag{5.23}$$

Experimental data for fully developed turbulent flames suggest that the turbulent burning velocity is approximately $s_T = 2v'$ for $v' \gg s_L^0$ in the large-scale turbulence limit (Abdel-Gayed & Bradley 1981). Using (4.1) it follows that $\tilde{\sigma}_t = 2v'/s_L^0$ and therefore

$$c_2\, c_4 = 0.39\, c_1. \tag{5.24}$$

Similarly, for the thin reaction zones regime we have the balance

$$c_3\, D\tilde{\sigma}_t^2 = c_1\, D_t. \tag{5.25}$$

Here we follow Damköhler (1940) who believed that the constant of proportionality in (1.9) should be unity and set

$$c_3 = c_1. \tag{5.26}$$

In order to define the laminar flame thickness unambiguously in the present context we also set

$$D = s_L^0 \ell_F. \tag{5.27}$$

Then (5.22) leads to the quadratic equation

$$\tilde{\sigma}_t^2 + 0.39\frac{\ell}{\ell_F}\tilde{\sigma}_t - 0.78\frac{v'\ell}{s_L^0\ell_F} = 0 \tag{5.28}$$

with the solution

$$\tilde{\sigma}_t = -\frac{0.39}{2}\frac{\ell}{\ell_F} + \left(\left(\frac{0.39}{2}\frac{\ell}{\ell_F}\right)^2 + 0.78\frac{v'\ell}{s_L^0\ell_F}\right)^{1/2}. \tag{5.29}$$

This equation satisfies the limits $\ell/\ell_F \to \infty$ corresponding to $\tilde{\sigma}_t = 2v'/s_L^0$ for the corrugated flamelets regime and $\ell/\ell_F \to 0$ corresponding to $\tilde{\sigma}_t = (D_t/D)^{1/2}$ for the thin reaction zones regime. Using (4.1) and (5.3) we now express the turbulent burning velocity as

$$s_T = s_L^0(1 + \tilde{\sigma}_t). \tag{5.30}$$

In figure 5 the ratio of the turbulent to the laminar burning velocity has been plotted using (5.29) and (5.30) for lengthscale ratios ℓ/ℓ_F ranging from 1 to 100. A constant lengthscale ratio is typical for experiments at constant pressure with a fixed geometry. Figure 5 thus shows the 'bending' behaviour of the turbulent burning velocity as v'/s_L^0 increases. It corresponds to the deviation from the straight line $s_T = s_L^0 + 2v'$ and leads to smaller values of s_T/s_L^0 for small lengthscale ratios.

The burning velocity diagram may also be plotted with the Reynolds number as a parameter. Such correlations have been plotted in Abdel-Gayed & Bradley (1981)

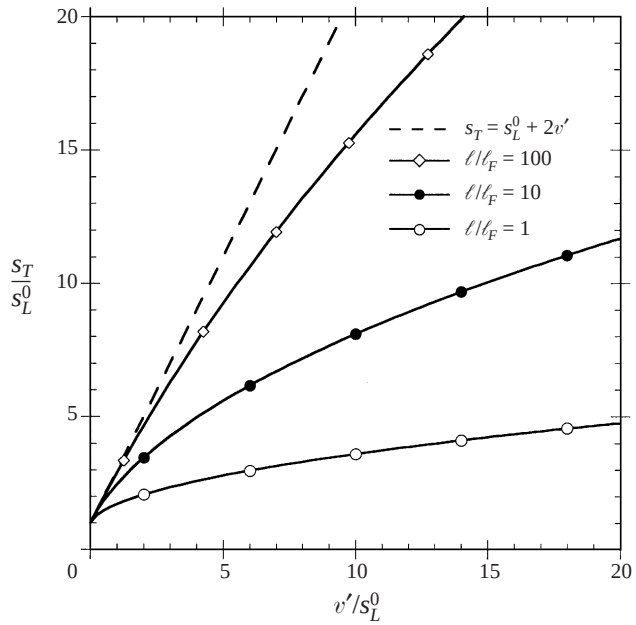

FIGURE 5. Ratio of the turbulent to the laminar burning velocity as a function of v'/s_L^0 for different lengthscale ratios ℓ/ℓ_F.

for Reynolds numbers ranging from $Re < 25$ to $Re = 4600$. However, it must be recognized that in many experiments quantitative information about lengthscales is missing. Also, in interpreting many experimental data the burning velocity was assumed to have reached its steady state while it may still have been developing. We use figures 7, 9 and 11 of Abdel-Gayed & Bradley (1981) and assign the average Reynolds number values of 1250, 625 and 300, based on the definition (2.5), to these figures, respectively. The comparison between the curves calculated from (5.29) and (5.30) and the experimental data collected in Abdel-Gayed & Bradley (1981) is shown in figure 6. Although the scatter of the data is quite considerable the calculated burning velocities seem to follow the trend in the data.

In closing this section it should be noted that the flame surface area ratio $\bar{\sigma}$ is related to the flame surface density Σ used by Trouvé & Poinsot (1994) as

$$\bar{\sigma} = \int_{-\infty}^{+\infty} \Sigma(x_n)\,\mathrm{d}x_n, \tag{5.31}$$

where $x_n = \boldsymbol{n}\cdot\boldsymbol{x}$ is the coordinate normal to the flame brush. A model equation for Σ proposed by Trouvé & Poinsot (1994) also contains a production term proportional to Σ and a sink term proportional to $s_L\,\Sigma^2$. It therefore describes the kinematic restoration of flame surface area ratio, valid in the corrugated flamelets regime. Since it does not explicitly contain a term proportional to $D\,\Sigma^3$ it does not describe the physics in the thin reaction zones regime and cannot recover Damköhler's limit of small-scale turbulence.

6. Discussion

It is the aim of the present paper to extend the flamelet approach beyond the corrugated flamelets regime into a regime which now is called the thin reaction zones

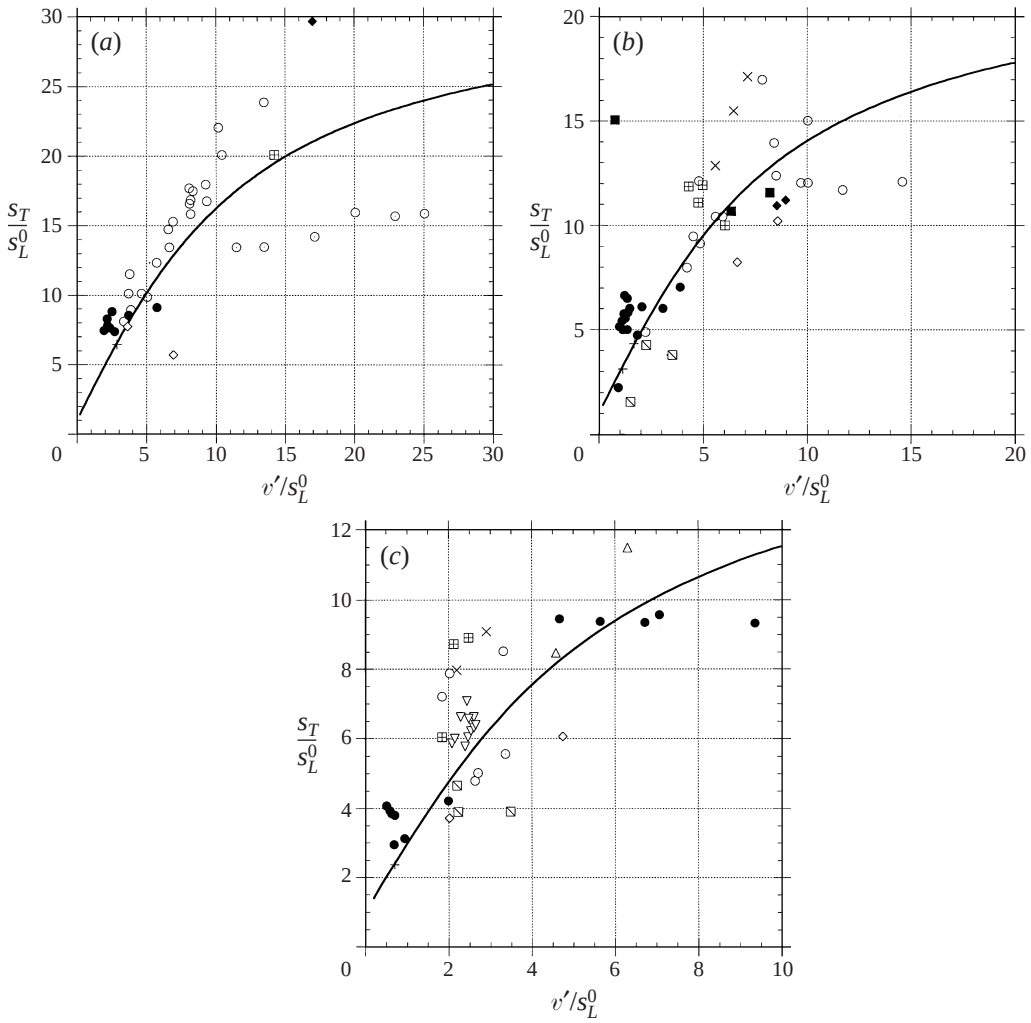

FIGURE 6. Comparison of the burning velocity ratio calculated from (5.29) and (5.30) (solid lines) with data by Abdel-Gayed & Bradley (1981) (the origin of the individual data points may be found in that reference). (*a*) $Re = 1250$ (calculated) and ranging between 1000 and 1500 (data); (*b*) $Re = 625$ (calculated) and ranging between 500 and 750 (data); (*c*) $Re = 300$ (calculated) and ranging between 250 and 350 (data).

regime. It can be shown that the reaction zone represents a surface within the flow similar to the flame front in the corrugated flamelets regime. This property could be exploited to apply the level-set approach. In this formulation the curvature term rather than the propagation term becomes dominant. The curvature term contains the mass diffusivity rather than the Markstein diffusivity. The latter appears in the curvature term in the corrugated flamelets regime, but there it is a higher-order term and may be neglected to leading order. As a consequence of this leading-order analysis the Markstein length and thereby the Lewis number does not enter into the formulation. This simplification may lead to inaccuracies at the border line between the corrugated flamelets regime and the thin reaction zones regime where the propagation term and the curvature term are of the same order of magnitude.

In the derivation of the kinematic and the diffusive *G*-equation gas expansion

effects in the flame front were not taken into account. These effects are known to be important at values of v'/s_L^0 up to around 3 where they generate countergradient diffusion of the progress variable (Bray 1996). Also associated with gas expansion are flame front instabilities known as the Darrieus–Landau instability. These effects need to be implemented into the level-set-approach. They become relatively less important for values of v' that are much larger than the gas expansion velocity which scales with s_L^0. Therefore, in the thin reaction zones regime they are expected to be unimportant, but they need to be addressed in the corrugated flamelets regime. This will be done in a forthcoming paper.

7. Conclusions

While the laminar burning velocity is the principle scaling quantity for the corrugated flamelets regime, the diffusion coefficient takes this role in the thin reaction zones regime. Based on a level-set formulation for both regimes it could be shown that this manifests itself by scalar dissipation in the thin reaction zones regime rather that by kinematic restoration, as in the corrugated flamelets regime. Although both mechanisms act in the same way in both regimes in limiting scalar fluctuations and thereby the flame brush thickness, their effect on the flame surface area ratio $\tilde{\sigma}$ is quite different. A model equation for the flame surface area ratio increase by turbulence $\tilde{\sigma}_t$ was derived for both regimes showing that kinematic restoration of $\tilde{\sigma}_t$ scales like $\tilde{\sigma}_t^2$, while scalar dissipation scales like $\tilde{\sigma}_t^3$. As an immediate result of these scalings one recovers Damköhler's turbulent burning velocity expressions as limiting cases for the large-scale and the small-scale turbulence regimes, respectively.

Appendix

We want to derive closure relations for the sink terms $\tilde{\omega}$ and $\tilde{\chi}$ in (4.7). In modelling non-constant-density turbulence it is generally assumed that closure models derived for constant-density turbulence can also be used for Favre-averaged equations (Jones 1994). Therefore, for simplicity, we assume constant density and consider the special case of homogeneous isotropic turbulence. This corresponds to an ensemble of thin reaction zones propagating in all directions within a given spatial domain. We shall consider the two-point correlation between $G'(\boldsymbol{x},t)$ at $\boldsymbol{x}$ and $G'(\boldsymbol{x}+\boldsymbol{r},t)$ at $\boldsymbol{x}+\boldsymbol{r}$ defined as

$$g^2(\boldsymbol{r},t) = \overline{G'(\boldsymbol{x},t)\,G'(\boldsymbol{x}+\boldsymbol{r},t)} \tag{A 1}$$

and proceed in the same way as Peters (1992) by transforming the resulting two-point correlation equation

$$\frac{\partial g^2}{\partial t} + 2\,\frac{\partial \overline{v'_\alpha(\boldsymbol{x}+\boldsymbol{r},t)G'(\boldsymbol{x},t)G'(\boldsymbol{x}+\boldsymbol{r},t)}}{\partial r_\alpha} - 2s_L^0\,\overline{G'(\boldsymbol{x}+\boldsymbol{r},t)\sigma'(\boldsymbol{x},t)} + 2D\,\overline{\sigma'(\boldsymbol{x}+\boldsymbol{r},t)\sigma'(\boldsymbol{x},t)} = 0 \tag{A 2}$$

into Fourier space. This leads to an equation for the scalar spectrum function

$$\Gamma(k,t) = 4\pi k^2 \hat{g}^2 \tag{A 3}$$

where the $\hat{}$ denotes the Fourier transform and k is the wavenumber.

Since the two-point correlation corresponding to the kinematic restoration is non-linear its Fourier transform will contain contributions from all wavenumbers k. As in Peters (1992) we will use the gradient transport assumption of Pao (1965, 1968) and

assume localness of interactions (cf. Frisch 1995, p. 104) for the turbulent transport term and for the term corresponding to the kinematic restoration. This means that these quantities are functions of the local wavenumber k only rather than of the entire wavenumber spectrum. Using dimensional analysis one realizes that all these terms have the dimension [$\mathrm{g^2\,s^{-1}}$]. Closure of these terms therefore suggests that they should be linear in $\Gamma(k,t)$. Similar to the previous analysis this leads to the following equation for the spectrum function

$$C_s\frac{\partial\Gamma}{\partial t}+\bar{\varepsilon}^{1/3}\left(\tfrac{5}{3}k^{2/3}\Gamma+k^{5/3}\frac{\partial\Gamma}{\partial k}\right)+c_1\,s_L^0\,k\Gamma+c_2D\,k^2\Gamma=0, \tag{A 4}$$

which has the solution

$$\Gamma(k,t)=C_s\overline{\chi}_0\bar{\varepsilon}^{-1/3}H(k_0(t))k^{-5/3}\exp(-3c_1(\ell_G k)^{1/3})\exp(-\tfrac{3}{4}c_2(\ell_C k)^{4/3}). \tag{A 5}$$

Here C_s is the universal constant of the scalar spectrum and $\overline{\chi}_0$ is a reference value for the scalar dissipation rate. For simplicity of the subsequent calculations we have assumed an abrupt small-wavenumber cut-off at the integral scale by introducing the Heaviside function $H(k_0(t))$ where $k_0=\ell^{-1}$. This spectrum is similar to that in (3.13) of Peters (1992) except that the last exponential term which modelled the strain term has disappeared. Also, since the dissipation term now corresponds to the classical scalar dissipation, it is linear and the empirical coefficient c_2 of Peters (1992) is equal to $c_2=2C_s$. For $\ell^{-1}<k<\ell_C^{-1}<\ell_G^{-1}$ the exponential terms approach unity and one obtains the classical $-5/3$ spectrum for the inertial range.

The Gibson scale ℓ_G appearing in (A 5) influences the spectrum function only at large wavenumbers because in the thin reaction zones regime it is smaller than the Obukhov–Corrsin scale ℓ_C. Therefore kinematic restoration acts merely as an additional mechanism to reduce the scalar fluctuations. For $k\gg\ell_G^{-1}$ this term may be neglected. We linearize the remaining exponential terms in (A 5) to obtain in the vicinity of ℓ_C the form

$$\Gamma(k,t)=\frac{C_s\overline{\chi}_0H(k_0(t))}{\bar{\varepsilon}^{1/3}k^{5/3}+\frac{3}{2}C_sDk^3}\,. \tag{A 6}$$

The two terms in the denominator illustrate that the scalar spectrum is determined by the turbulent flow field through $\bar{\varepsilon}$ for $k<\ell_C^{-1}$ and by diffusion for $k>\ell_C^{-1}$.

Equation (A 4) may be integrated over k between $k=k_0$ and $k=\infty$. The spectral transfer term then vanishes and one obtains the analogue of (4.7) for constant-density homogeneous isotropic turbulence

$$\frac{\partial\overline{G'^2}}{\partial t}=-\overline{\omega}-\overline{\chi}\,. \tag{A 7}$$

The terms in these equations are defined as

$$\overline{G'^2}=\int_{k_0}^{\infty}\Gamma(k)\,\mathrm{d}k, \tag{A 8}$$

$$\overline{\omega}=C_s^{-1}\,c_1\,s_L^0\int_{k_0}^{\infty}k\Gamma\;\mathrm{d}k \tag{A 9}$$

and

$$\overline{\chi}=2D\int_{k_0}^{\infty}k^2\Gamma\;\mathrm{d}k. \tag{A 10}$$

These integrals may be evaluated in order to derive closure relations that relate $\overline{\omega}$ and $\overline{\chi}$ to $\overline{G'^2}$ and the parameters ℓ and $\bar{\varepsilon}$ describing the flow field.

Since the diffusive cut-off occurs at ℓ_C we introduce the variable

$$y = \tfrac{3}{4}\, c_2(\ell_C k)^{4/3} \tag{A 11}$$

to obtain the scalar dissipation by integrating (A 10) as

$$\overline{\chi} = \overline{\chi}_0 I_1 \tag{A 12}$$

with

$$I_1 = \int_{y_0}^{\infty} \exp\left(-y - \gamma^{1/3} y^{1/4}\right) \mathrm{d}y, \tag{A 13}$$

where the small-wavenumber cut-off at $k = k_0$ was introduced which leads with (A 11) to

$$y_0 = \tfrac{3}{4} c_2 \left(\frac{\ell_C}{\ell}\right)^{4/3}, \tag{A 14}$$

where ℓ/ℓ_C is a measure for the inertial range of the scalar spectrum. Furthermore

$$\gamma = \left(\frac{108\, c_1^4}{c_2}\right)^{3/4} \frac{\ell_G}{\ell_C} \tag{A 15}$$

is proportional to the ratio of ℓ_G/ℓ_C which should be small in the thin reaction zones regime. The integral can be expanded for small values of $\gamma^{1/3}$ and y_0 as

$$I_1 = 1 - \gamma^{1/3} \Gamma\left(\tfrac{5}{4}\right) - y_0, \tag{A 16}$$

where Γ is the gamma function. Equation (A 16) shows that in the limit $\gamma \to 0$, $y_0 \to 0$, $\overline{\chi}$ is equal to $\overline{\chi}_0$.

Similarly, we can integrate (A 8) to obtain

$$\overline{G'^2} = \tfrac{3}{2} C_s \overline{\chi} \varepsilon^{-1/3} \ell^{2/3} \frac{I_2}{I_1}, \tag{A 17}$$

where the integral

$$I_2 = \tfrac{1}{2} y_0^{1/2} \int_{y_0}^{\infty} y^{-3/2} \exp\left(-y - \gamma^{1/3} y^{1/4}\right) \mathrm{d}y \tag{A 18}$$

can be expanded in the limit $\gamma \to 0$, $y_0 \to 0$ as

$$I_2 = 1 - (\pi)^{1/2} y_0^{1/2} + y_0 - 2\gamma^{1/3} y_0^{1/4}. \tag{A 19}$$

Equation (A 17) relates the scalar dissipation $\overline{\chi}$ to $\overline{G'^2}$. If we use (2.1) for the turbulent kinetic energy, (5.17) for the integral length scale as well as $C_s = 1.2$, which is the value preferred by Monin & Yaglom (1987), we obtain for $\gamma \to 0$, $y_0 \to 0$

$$\overline{\chi} = c_\chi \frac{\bar{\varepsilon}}{\bar{k}} \overline{G'^2} \tag{A 20}$$

with $c_\chi = 1.62$. This relation is identical to (4.3) for the kinematic restoration obtained by Peters (1992) for the corrugated flamelets regime. Here, in the thin reaction zones regime, we recover with (A 20) the classical closure relation for diffusive scalars.

The kinematic restoration can be related to the scalar dissipation as

$$\overline{\omega} = \overline{\chi} \gamma^{1/3} \Gamma\left(\tfrac{5}{4}\right) \frac{I_3}{I_1}, \tag{A 21}$$

where I_3 is defined as

$$I_3 = \frac{1}{4\Gamma(\frac{5}{4})}\int_{y_0}^{\infty} y^{-3/4}\exp(-y-\gamma^{1/3}y^{1/4})\,\mathrm{d}y, \tag{A 22}$$

which can be expanded for $\gamma \to 0$, $y_0 \to 0$ as

$$I_3 = 1 - y_0^{1/4}e^{-y_0}/\Gamma(\tfrac{5}{4}) - \gamma^{1/3}\Gamma(\tfrac{3}{2})/(2\Gamma(\tfrac{5}{4})). \tag{A 23}$$

Since $\gamma^{1/3}$ may be expressed as

$$\gamma^{1/3} = \left(108/c_2\right)^{1/4} c_1\,(s_L^0/v_\eta)Pr^{1/4} \tag{A 24}$$

(A 21) shows that the ratio of the kinematic restoration to the scalar dissipation in the thin reaction zones regime is proportional to the ratio of the laminar burning velocity s_L^0 to the Kolmogorov velocity v_η. It is interesting to compare this ratio with that obtained previously for the corrugated flamelets regime by Peters (1992), which, in the limit $\gamma \to \infty$, when written in the present notation, is

$$\overline{\chi} = 24\gamma^{-4/3}\overline{\omega}, \tag{A 25}$$

where $\overline{\omega}$ is given by (4.3).

For modelling purposes we may now construct formulae that satisfy the limiting expressions (A 21) with $I_3/I_1 = 1$ and (A 25) and could therefore be used for calculations that cover both regimes of premixed turbulent combustion. These are

$$\overline{\chi} = F_\chi(\gamma^{4/3})c_\chi(\bar{\varepsilon}/\bar{k})\overline{G'^2}\,, \quad \overline{\omega} = F_\omega(\gamma^{1/3})c_\omega(\bar{\varepsilon}/\bar{k})\overline{G'^2} \tag{A 26}$$

with

$$F_\chi = \frac{24}{24+\gamma^{4/3}}\,, \quad F_\omega = \frac{\Gamma(\frac{5}{4})\gamma^{1/3}}{1+\Gamma(\frac{5}{4})\gamma^{1/3}}. \tag{A 27}$$

Since the sum of F_χ and F_ω varies for γ ranging from $\gamma = 0$ to $\gamma \to \infty$ between a maximum value of 1.45 and a minimum value of 0.88 we propose replacing $F_\chi + F_\omega$ by a constant c^* and write

$$\overline{\omega} + \overline{\chi} = c_s(\bar{\varepsilon}/\bar{k})\overline{G'^2}, \tag{A 28}$$

where $c_s = c^*c_\chi = 2.0$.

REFERENCES

Abdel-Gayed, R. G. & Bradley, D. 1981 A two-eddy theory of premixed turbulent flame propagation. *Phil. Trans. R. Soc. Lond.* A **301**, 1–25.

Borghi, R. W. 1985 On the structure and morphology of turbulent premixed flames. In *Recent Advances in the Aerospace Science* (ed. C. Casci), pp. 117–138. Plenum.

Bradley, D. 1992 How fast can we burn? In *Twenty-Fourth Symp.* (*Intl*) *on Combustion*, pp. 247–262. The Combustion Institute.

Bray, K. N. C. 1990 Studies of the turbulent burning velocity. *Proc. R. Soc. Lond.* A **431**, 315–335.

Bray, K. N. C 1996 The challenge of turbulent combustion. In *Twenty-Sixth Symp.* (*Intl*) *on Combustion*, pp. 1–26. The Combustion Institute.

Bray, K. N. C. & Peters, N. 1994 Laminar flamelets in turbulent flames. In *Turbulent Reacting Flows* (ed. P. A Libby & F. A. Williams), pp. 63–113. Academic.

Chen, Y.-C. 1994 Measurements of the inner layer temperature in highly stretched turbulent flames. PhD thesis, RWTH Aachen (in English).

Chen, Y.-C., Peters, N., Schneemann, G. A., Wruck, N., Renz, U. & Mansour, M. S. 1996 The detailed flame structure of highly stretched turbulent premixed methane-air flames. *Combust. Flame* **107**, 223–244.

Damköhler, G. 1940 Der Einfluß der Turbulenz auf die Flammengeschwindigkeit in Gasgemischen. *Z. Elektrochem.* **46**, 601–652. (English translation *NASA Tech. Mem.* 1112, 1947).

Echekki, T. & Chen, J. H. 1996 Unsteady strain rate and curvature effects in turbulent premixed methane-air flames. *Combust. Flame* **106**, 184–202.

Echekki, T. & Chen, J. H. 1998 Analysis of the contribution of curvature to premixed flame propagation. Submitted to *Combust. Flame.*

Frisch, U. 1995 *Turbulence*. Cambridge University Press.

Gibson, C. H. 1968 Fine structure of scalar fields mixed by turbulence I. Zero gradient points and minimal gradient surfaces. *Phys. Fluids* **11**, 2305–2315.

Jones, W. P. 1994 Turbulence modelling and numerical solution methods for variable density and combusting flows. In *Turbulent Reacting Flows* (ed. P. A. Libby & F. A. Williams), pp. 309–374. Academic.

Joulin, G. 1994 On the response of premixed flames to time-dependent stretch and curvature. *Combust. Sci. Tech.* **97**, 219–229.

Kerstein, A. R., Ashurst, Wm. T. & Williams, F. A. 1988 Field equation for interface propagation in an unsteady homogeneous flow field. *Phys. Rev.* A **37**, 2728–2731.

Matalon, M. & Matkowsky, B. J. 1982 Flames as gasdynamic discontinuities. *J. Fluid Mech.* **124**, 239–259.

Monin, A. S. & Yaglom, A. M. 1987 *Statistical Fluid Mechanics: Mechanics of Turbulence*, vol. 2, MIT Press.

Pao, Y. H. 1965 Structure of turbulent velocity and scalar fields at large wave numbers. *Phys. Fluids* **8**, 1063–1065.

Pao, Y. H. 1968 Transfer of turbulent energy and scalar quantities at large wavenumbers. *Phys. Fluids* **11**, 1371–1372.

Pelce, P. & Clavin, P. 1982 Influence of hydrodynamics and diffusion upon the stability limits of laminar premixed flames. *J. Fluid Mech.* **124**, 219–237.

Peters, N. 1986 Laminar flamelet concepts in turbulent combustion. In *Twenty-First Symp.* (*Intl*) *on Combustion*, pp. 1231–1250. The Combustion Institute.

Peters, N. 1991 Length scales in laminar and turbulent flames. In *Numerical Approaches to Combustion Modelling* (ed. S. Oran & J. P. Boris). *Progr. Astronaut. Aeronaut.* **135**, 155–182.

Peters, N. 1992 A spectral closure for premixed turbulent combustion in the flamelet regime. *J. Fluid Mech.* **242**, 611–629.

Peters, N. 1997 Kinetic foundation of thermal flame theory. In *Advances in Combustion Science: In Honor of Ya. B. Zel'dovich* (ed. W. A. Sirignano, A. G. Merzhanov & D. de Luca). *Progr. Astronaut. Aeronaut.* **173**, 73–91.

Peters, N., Terhoeven, P., Chen, J. H. & Echekki, T. 1997 Statistics of flame displacement speeds from computations of 2-D unsteady methane-air flames. *To be Presented at the 27th Symp.* (*Intl*) *on Combustion.* The Combustion Institute.

Pocheau, A. 1992 Front propagation in a turbulent medium. *Europhys. Lett.* **20**, 401–406.

Poinsot, T., Veynante, D. & Candel, S. 1991 Quenching process and premixed turbulent combustion diagrams. *J. Fluid Mech.* **228**, 561–605.

Seshadri, K. 1996 Multistep asymptotic analyses of flame structures. In *Twenty-Sixth Symp.* (*Intl*) *on Combustion*, pp. 831–846. The Combustion Institute.

Sivashinsky, G. I. 1977 Non-linear analysis of hydrodynamic instability in laminar flames I. Derivation of basic equations. *Acta Astronautica* **4**, 1177–1206.

Sussman, M., Fatemi, E. & Osher, S. 1994 A level set approach for computing solutions to incompressible two-phase flows. *J. Comput. Phys.* **114**, 146–159.

Trouvé, A. & Poinsot, Th. 1994 The evolution equation for the flame surface density in turbulent premixed combustion. *J. Fluid Mech.* **278**, 1–31.

Ulitsky, M. & Collins, L. R. 1997 Relative importance of coherent structures vs. background turbulence in the propagation of a premixed flame. *Combust. Flame* **111**, 257–275.

Williams, F. A. 1985*a Combustion Theory* (2nd Edition). Addison-Wesley.

Williams, F. A. 1985*b* Turbulent combustion. In *The Mathematics of Combustion* (ed. J. Buckmaster), pp. 97–131. SIAM.

Zel'dovich, Y. B. & Frank-Kamenetzkii, D. A. 1938 A theory of thermal propagation of flame. *Acta Physiochimica URSS IX*, 341–350.

Zimont, V. L. 1979 Theory of turbulent combustion of a homogeneous fuel mixture at high Reynolds numbers. *Combust. Expl Shock Waves* **15**, 305–311.